Ferromagnetic phases of bcc and fcc Fe, Co, and Ni

V. L. Moruzzi and P. M. Marcus
IBM Thomas J. Watson Research Center, P. O. Box 218, Yorktown Heights, New York 10598

K. Schwarz and P. Mohn
Institute of Technical Electrochemistry, Technical University of Vienna, A-1060 Vienna, Austria
(Received 5 March 1986)

The different magnetic phases of the bcc and fcc forms of Fe, Co, and Ni are studied by analyzing total-energy surfaces in moment-volume parameter space obtained from energy-band calculations using a local-spin-density approximation. The surfaces, found by calculating total energies while holding both the magnetic moment and the volume fixed, offer a method for studying phases that are inaccessible to traditional self-consistent-field methods. We find that magnetic moments can change discontinuously with volume and that there are ranges of coexistence for different magnetic phases. In the multiphase ranges, these elemental magnetic systems exhibit metamagnetic behavior. Our results show that bcc Co is ferromagnetic for all volumes studied, that fcc Co can exist in either a nonmagnetic or a ferromagnetic phase, and that there is a range of volumes where the two phases can coexist. For Fe, the bcc form exhibits a stable ferromagnetic phase for all volumes considered, but the fcc form can exist in any of three phases—a nonmagnetic, a low-spin, and a high-spin phase—all of which can coexist in limited volume ranges. For Ni, the fcc form exhibits a stable ferromagnetic phase, but the bcc form can exist in both a nonmagnetic and, at expanded volumes, a ferromagnetic phase. The volume ranges for all magnetic phases are clearly identified for the bcc and fcc forms of Fe, Co, and Ni.

I. INTRODUCTION

Use of the local-density approximation[1] (LDA) to account for exchange and correlation effectively reduces the many-body quantum-mechanical problem of the behavior of the electrons associated with a crystalline array of atoms to the solution of a set of coupled one-electron equations with periodic boundary conditions. Self-consistent electronic structure calculations utilizing the LDA are the basic theoretical tool used to study condensed systems. Accurate determinations of the total energy E as a function of the atomic separation or volume V yield binding curves which determine the ground state of a system of atoms. We note that the system is in equilibrium at zero pressure only at volumes corresponding to the minima of the energy. At other volumes the system is under the influence of an external pressure. Thus, the effect of an external applied pressure P (positive or negative) is simulated by forcing the system to have a given volume. Systematic studies of the changes in total energy as a function of volume yield theoretical ground-state properties such as equilibrium volumes, cohesive energies, and bulk moduli for the cubic metallic elements which are in essential agreement with experiment.[2]

The local-spin-density approximation (LSDA) is a spin-polarized form of the LDA which allows the extension of electronic structure calculations, and the study of the resulting ground-state properties including magnetic moments, to the magnetic elements.[2–4] Previous studies of the magnetic elements have been based on the analysis of binding curves (total energy versus volume) obtained from "standard" spin-polarized calculations. Such calculations involve the simultaneous determination of both the total energy and the magnetic moment. The resulting binding curves therefore contain a hidden variable, namely the magnetic moment. Such curves, particularly for fcc Fe,[3,4] indicate that a magnetic collapse or a breakdown of ferromagnetism occurs at certain volumes and implies the existence of more than one magnetic phase. However, the actual behavior in the breakdown region or the ranges of existence and degrees of stability of various phases are not clear in this earlier work.

In the present work, we study bcc and fcc Fe, Co, and Ni using a new fixed spin-moment method[5] which yields the ground state of a constrained system.[6] In this method, the total energy of a system is determined with a fixed volume per atom, V, and a fixed magnetic moment per atom, M, (i.e., M is constrained to have a given value). In this case, the total-energy function is determined in a parameter space of M and V, resulting in a binding surface. True equilibrium corresponds to M and V loci where the pressure $P=-(\partial E/\partial V)_M$ and an external applied magnetic field $H=(\partial E/\partial M)_V$ are both zero. Other points on the binding surface correspond to total energies at finite applied pressure or magnetic field. Thus, forcing the magnetic moment to have a given (nonequilibrium) value simulates an applied field in the same way that forcing the system to have a given volume simulates an applied pressure.

Standard spin-polarized and fixed spin-moment calculations have interesting similarities and differences. Both methods involve the determination of total energies for a fixed volume. Standard spin-polarized calculations yield

a *curve* of the total energy as a function of volume with different points along the curve corresponding to different moments. The magnetic field H is fixed (usually implicitly assumed to be zero) and the magnetic moment is allowed to float until the energy is minimized. In the fixed spin-moment method, the magnetic moment is fixed, and the magnetic field is determined from the moment derivative of the total energy at constant volume. Fixed spin-moment calculations yield total energies in moment-volume space, or a binding *surface,* where the magnetic field has the same relation to the magnetic moment that the pressure has to the volume.

Since the fixed spin-moment method surveys an entire surface it requires many more calculations than standard spin-polarized calculations. Fixed spin-moment calculations, however, achieve self-consistency more rapidly than floating moment calculations and are not plagued by convergence difficulties commonly encountered in standard calculations for systems which exhibit large changes in magnetic moment with small changes in total energy. As a consequence, binding surfaces yield much more detailed information and give a global view of the different phases available to the system. We will show that analysis of binding surfaces yields the conditions required for the stability of different magnetic phases.

In the following sections, we briefly discuss the method used, the approximations involved, and the reliability of the results. We show that the spin-moment method yields details beyond those of the standard spin-polarized method and gives a unified view of the different magnetic phases of bcc and fcc Fe, Co, and Ni. We present binding surfaces $E(M,V)$ for bcc and fcc Fe, show detailed evidence for the existence of a nonmagnetic, low-spin and high-spin phase for fcc Fe, and give field contour surfaces $H(M,V)$ which show the ranges of existence for the different magnetic phases of the magnetic elements and discuss the expected metamagnetic behavior. Finally, we make a critical comparison of our results and the results of previous work.

II. ENERGY SURFACES

All work presented here is based on the augmented-spherical-wave method of Williams, Kübler, and Gelatt,[7] which assumes a spherical effective potential within each Wigner-Seitz sphere and uses the LSDA as formulated by von Barth and Hedin[8] and modified by Janak,[9] to account for exchange and correlation. The calculations are nonrelativistic and are done on a uniform mesh of 570 points for the fcc and 405 points for the bcc irreducible $\frac{1}{48}$ wedge of the Brillouin zone. The reliability of the basic computations is established by the general agreement between calculated and experimental values for cohesive energies, equilibrium lattice constants, and bulk moduli for the $3d$ and $4d$ transition metals,[10] and, as we shall show, by finding that bcc Fe and fcc Co and Ni are more stable than fcc Fe and bcc Co and Ni, respectively, at zero pressure.

The primary information obtained from the energy-band calculations is the binding surfaces, or surfaces described by total-energy contours in the M-V plane. We replace the volume by the Wigner-Seitz radius r_{WS} ($V=4\pi r_{WS}^3/3$). Analysis of binding surfaces for Co (Refs. 11 and 12) shows that in the bcc form and in the range of r_{WS} values studied, Co exists only in the ferromagnetic (FM) phase, while in the fcc form it can be FM or nonmagnetic (NM) with a two-phase volume range accessible to both phases. The bcc form of Co has been prepared by Prinz,[13] who finds a lattice constant in good agreement with our calculated equilibrium ($P=0$) volume. For Ni (Ref. 12) the bcc and fcc forms are interchanged with respect to Co. The Ni fcc form shows a persistent FM phase and the bcc form shows FM and NM phases with no range of coexistence. In Figs. 1 and 2, we show the resulting binding surfaces for bcc and fcc Fe with contour lines at 1-mRy intervals. The surface for bcc Fe shows a deep FM minimum at a magnetic moment of $2.15\mu_B$ and $r_{WS}=2.63$ a.u. At zero pressure, bcc Fe would assume this locus, in agreement with experiment and with the results of previous standard spin-polarized calculations[2,14] utilizing the same form of the exchange-correlation potential. Curves of $E(M)$ at constant r_{WS} values yield a minimum at finite M values throughout the r_{WS} range studied, hence bcc Fe is magnetic throughout. The binding surface for fcc Fe (Fig. 2) is in sharp contrast to the bcc case (Fig. 1) and clearly shows a nonmagnetic

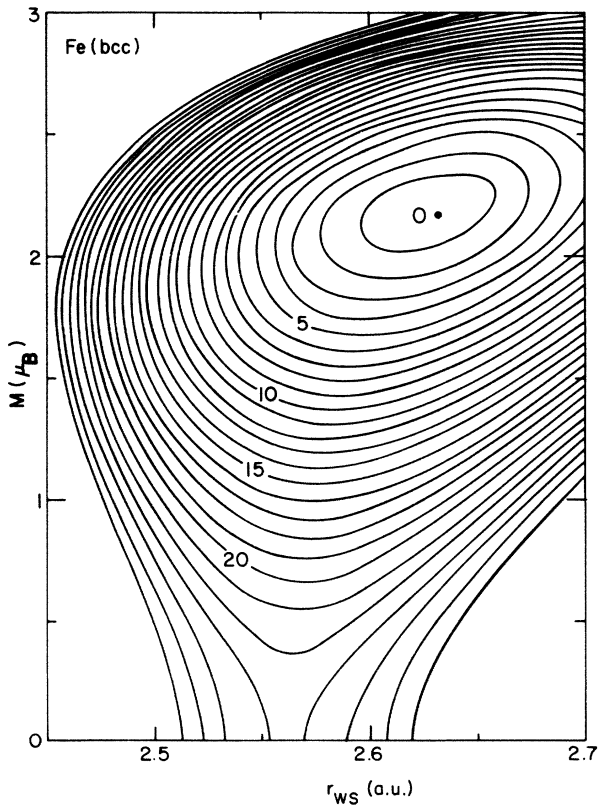

FIG. 1. Binding surface for Fe in the bcc structure. Contour lines are at 1-mRy intervals and are labeled relative to the minimum energy. The equilibrium point at $M=2.15\mu_B$ and $r_{WS}=2.63$ a.u. corresponds to $(\partial E/\partial M)_B=0$ (zero field) and $(\partial E/\partial V)_M=0$ (zero pressure). In the bcc structure, Fe is magnetic for all volumes considered.

phase at $M=0$ and $r_{WS}=2.54$ a.u. with the lowest energy. In addition, the fcc surface shows an obvious "trough" at high r_{WS} values and $M\simeq 2\mu_B$ and a region with almost vertical contour lines between. This complicated behavior is shown in detail in Fig. 3 where curves of $E(M)$ for selected r_{WS} are displayed. At $r_{WS}=2.69$ a.u., the deep ferromagnetic minimum at $M=2.4\mu_B$ represents the only stable phase. However, starting at $r_{WS}=2.685$ a.u. and well developed at $r_{WS}=2.68$ a.u. we find clear evidence for a second minimum at $M\simeq 1\mu_B$. As r_{WS} is decreased to 2.67 a.u., this second minimum becomes shallow and disappears and the system favors the nonmagnetic minimum ($M=0$), which persists to low r_{WS} values (the FM minimum disappears at lower r_{WS}). Figure 3, therefore, presents direct evidence for the existence of a NM, a low-spin (LS), and a high-spin (HS) phase for fcc Fe.

The behavior of $E(M)$ curves at fixed r_{WS} deduced from binding surfaces like Figs. 1 and 2 can be related to the behavior of the magnetic moment as a function of field. In Fig. 4 we give a schematic representation of four of the simplest forms the curves can have, along with the corresponding derivative curves $H(M)=(\partial E/\partial M)_V$. Although M is the independent variable in the calculation, we give the conventional magnetization curve by plotting $M(H)$. Curves of the type shown exhibit the metamagnetic behavior discussed by Wohlfarth and Rhodes, and by Shimizu.[15] The analysis of binding surfaces involves an explicit consideration of the details of the volume dependence of this metamagnetic behavior. Figure 4(a) with an energy minimum at $M=0$ shows $E(M)$ for a NM phase. Application of an external field is required for the system to display a magnetic moment, with the slope dM/dH giving the susceptibility. The $E(M)$ curve shown in Fig. 4(b) with an energy minimum at a finite M value represents the situation for a ferromagnetic system. Here, the system has a FM moment even at zero applied field and applying a field increases the moment. Note that the system is theoretically capable of sustaining a moment even with a negative (opposite to the direction of M) field.[16] At a certain negative "critical" field, an abrupt collapse of the moment occurs (the moment does not go to zero but flips to a direction parallel to the field). Figure 4(c) with a local minimum at $M=0$ and another minimum at a finite M value represents the next stage of complexity. The corresponding $M(H)$ curve now shows a

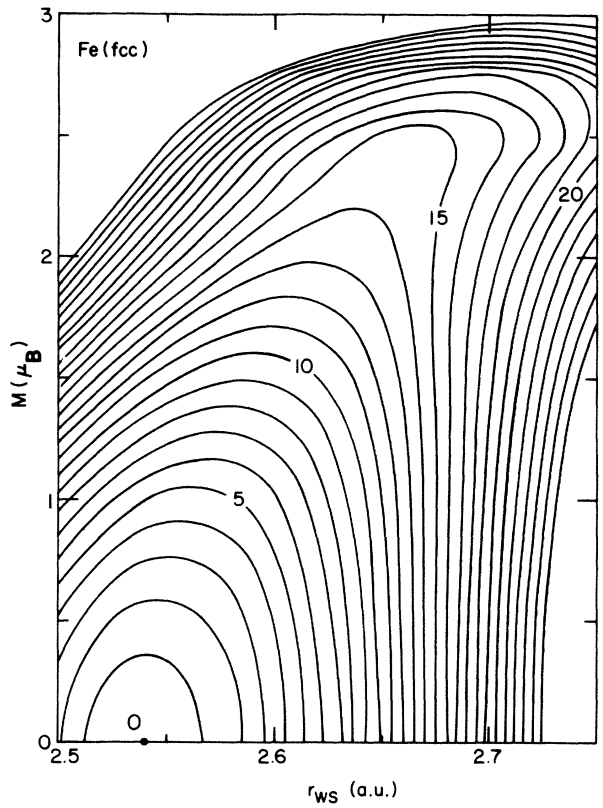

FIG. 2. Binding surface for Fe in the fcc structure. Contour lines are at 1-mRy intervals and are labeled relative to the minimum energy. The equilibrium point at $M=0$ and $r_{WS}=2.54$ a.u. indicates that fcc Fe is normally nonmagnetic. The "trough" at large volumes and magnetic moment is responsible for a high-spin magnetic phase which may be realized by clamping the system at high volumes. Detail analysis in the region of almost vertical contour lines (little variation of total energy with magnetic moment) also yields a second, low-spin magnetic phase.

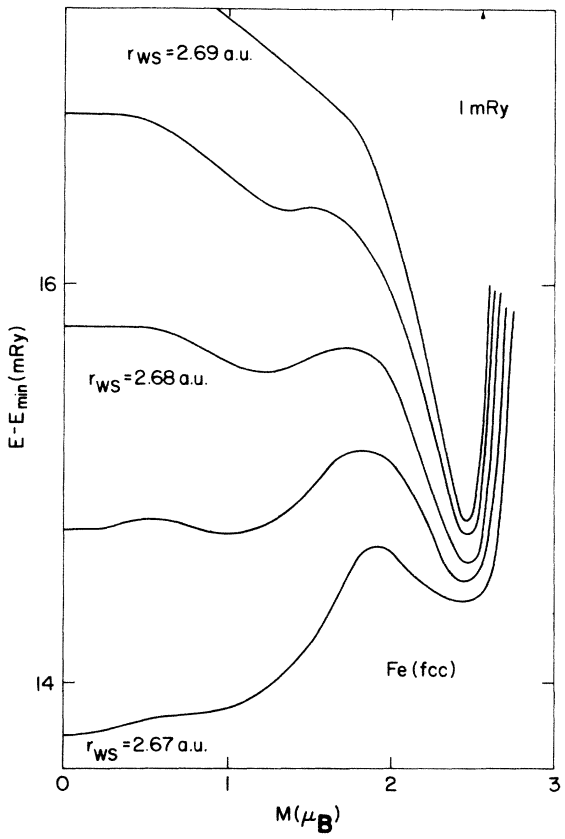

FIG. 3. Total energy (relative to a minimum energy) vs magnetic moment for fcc Fe at several r_{WS} values (volumes) in the coexistence region, showing the three phases. Note that at 2.67, the low-spin phase is only accessible by applying a magnetic field.

metamagnetic behavior. At zero field, the system is nonmagnetic. Application of a low field leads to an increase in moment (with a relatively high susceptibility) until a positive critical field is reached and the moment jumps discontinuously to a higher value (with a lower susceptibility). Decreasing the field to zero before reaching the critical value merely returns the moment to zero; decreasing the field to zero after having reached the critical value results in a finite moment and behavior similar to the ferromagnetic behavior represented in Fig. 4(b). The moment will persist even with a negative field until a negative critical field is reached (when the moment will flip to align with the field and assume either the high FM or the low NM value depending on the magnitudes of the two critical fields). The next stage of complexity is represented in Fig. 4(d) which has no energy minimum at the $M=0$ axis, but shows two minima at finite moment values (LS and HS). The $M(H)$ curve now shows that at zero field, the system is in the LS phase and that the moment increases with increasing field until at a critical field the system jumps to a HS phase and displays a susceptibility similar to an ordinary ferromagnet. The system retains a magnetic moment (HS or LS) even when the field is decreased to negative values. Note that in this case, three (one positive and two negative) critical fields are involved. In all cases, the dashed portions of the $M(H)$ curves represent regions that are inaccessible to the system.

III. FIELD CONTOURS

Magnetic phase information deduced from calculated binding surfaces and, especially, from $M(H)$ curves can be displayed in a number of ways. Field contour plots, found by forming $(\partial E/\partial M)_V$, are one of the ways of presenting this information. Figure 5 shows the field contours in 1-mRy/μ_B (2.35-MG) intervals for bcc Fe, derived from the energy surface shown in Fig. 1. The $H=0$ contour has special significance and corresponds to the loci of points found by the vertical tangents of the energy contours of Fig. 1. The resulting curve gives the magnetic moments (at $H=0$) as a function of r_{WS}. The position labeled $\times$ represents the zero-pressure point. The loci of

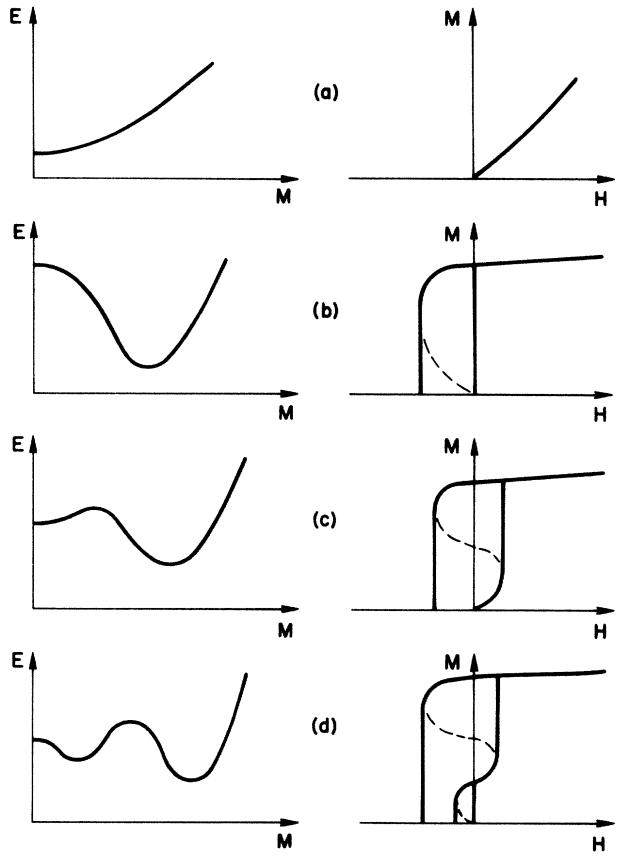

FIG. 4. Typical E-vs-M curves at selected volumes of binding surfaces like those of Figs. 1 and 2, along with the corresponding M-vs-H curves. For the curves in (a) and (b), the NM and the FM phase is stable, respectively. For (c), both phases are stable and the system exhibits metamagnetic behavior. In the case of (d), a LS and HS stable phase exists and the system can undergo a magnetic-metamagnetic transition.

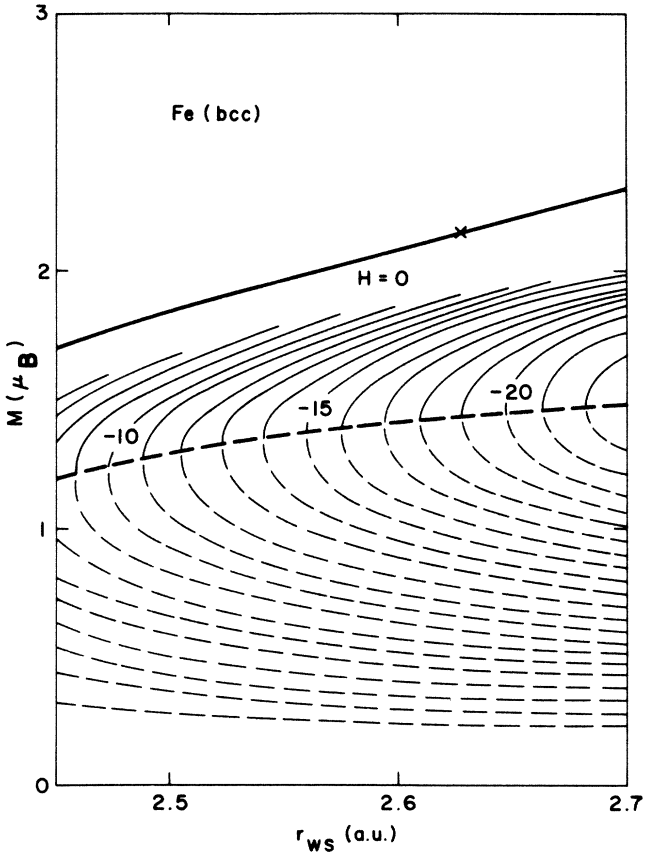

FIG. 5. Constant field contours for bcc Fe. The $H=0$ contour gives the moment-vs-r_{WS} curve and shows that the FM phase is stable throughout the range. The intersection of the contour lines and their vertical tangents defines the moment at the critical field where the susceptibility is infinite, and separates the accessible from the inaccessible (the region with dashed contour lines) region of the figure. The zero-pressure point is labeled $\times$.

vertical tangents to the field contours give the line on which $(\partial H/\partial M)_V = 0$. This is the line corresponding to the moments at the critical fields implied in Fig. 4(b). In all cases, this moment is less than the zero-field moment. Here, the critical field values are all negative and can be read directly off the figure. The dashed portions of the field contour lines correspond to the dashed portion of the $M(H)$ curve of Fig. 4(b) and are not accessible to the system. All moment values above the infinite susceptibility line are, however, accessible with an applied field greater than the indicated (volume-dependent) critical field.

Field contours derived from the binding surface[11] for fcc Co are shown in Fig. 6. In this case, the $H=0$ contour extends into the inaccessible (dashed) region. The solid portion of this $H=0$ contour gives the moment as a function of r_{WS}. Thus, fcc Co exists in the FM phase (can sustain a magnetic moment with no applied field) at all $r_{WS} \geq 2.47$ a.u., and is FM at zero pressure ($r_{WS}=2.58$ a.u.). As the figure shows, the system can exist in the NM phase at all $r_{WS} \leq 2.50$ a.u. Both phases are allowed in the range between 2.47 and 2.50 a.u. This is the metamagnetic range where the system behaves as shown in Fig. 4(c), showing an increasing low moment at low fields, an abrupt jump to a high moment at a certain positive critical field, and a retention of a high moment with a subsequent decrease in field until a negative critical field is reached (where the moment flips and aligns with the field). The line of infinite susceptibilities separating the accessible and inaccessible regions is multivalued and extends down to $r_{WS}=2.44$ a.u. In the range between $r_{WS}=2.44$ and 2.47 a.u. the FM phase is not stable. In this range, the system can be forced into the metamagnetic extension of the FM phase by applying a positive field exceeding a critical value. By decreasing the field below another positive critical value, however, the system returns to the NM phase. This metamagnetic range is shown by the heavy dashed line in the figure. We note that the curves specifying the zero-field moment, and the moment at the critical fields, both terminate with an infinite dM/dV.

As already mentioned and illustrated in Fig. 3, fcc Fe is capable of existing in a NM, a LS, and a HS phase. Field contours obtained from the binding surface represented in Fig. 2 are shown in Fig. 7. Although this figure is somewhat complicated, it contains a wealth of magnetic phase information. At zero pressure ($r_{WS}=2.54$ a.u.), it is NM. The system is capable of sustaining the NM phase at all $r_{WS} \leq 2.685$ a.u. At $r_{WS} \geq 2.66$ a.u., the ferromagnetic (HS) phase is stable. As shown in the figure, the LS phase with a moment ranging from $0.9\mu_B$ to $1.5\mu_B$ is also possi-

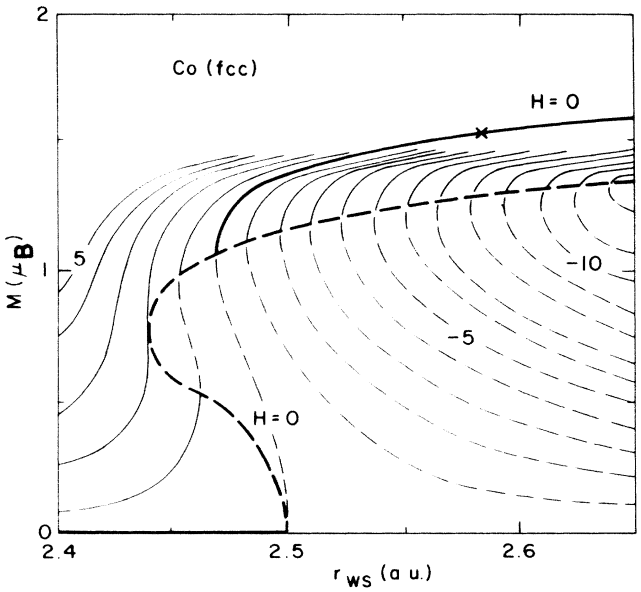

FIG. 6. Constant field contours for fcc Co exhibiting a stable FM phase for $r_{WS} \geq 2.47$ a.u., a stable NM phase for $r_{WS} \leq 2.50$ a.u., and a metamagnetic extension of the FM phase between 2.44 and 2.47 a.u. In the range between 2.47 and 2.50 a.u., fcc Co is metamagnetic and can exist in both the FM and NM phases. The heavy dashed line specifies the moments at the critical field values. The zero-pressure point is labeled $\times$.

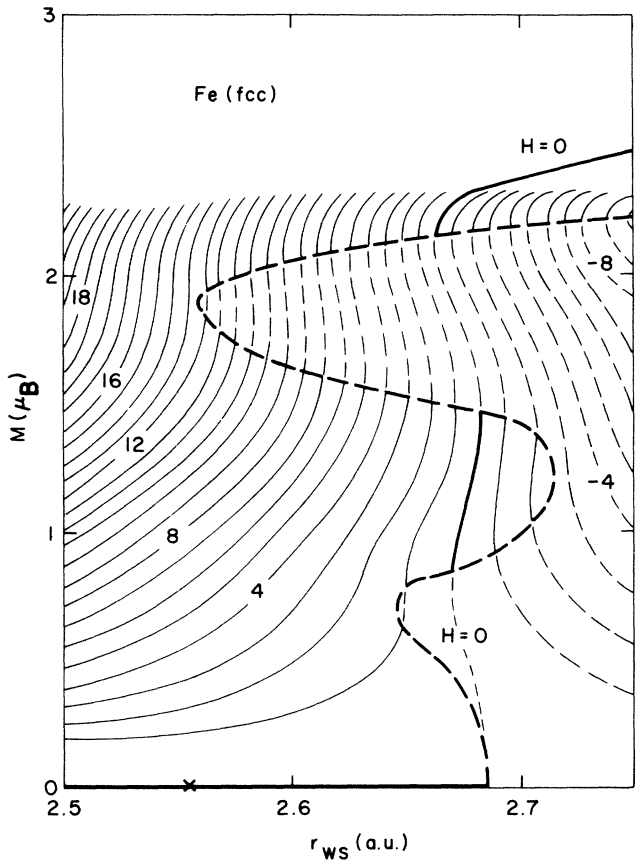

FIG. 7. Constant field contours for fcc Fe exhibiting a stable HS phase for $r_{WS} \geq 2.66$ a.u., a stable LS phase for r_{WS} between 2.670 and 2.685 a.u., and a stable NM phase for $r_{WS} \leq 2.685$ a.u. The metamagnetic extension of the HS phase is accessible between 2.56 and 2.66 a.u., while the metamagnetic extension of the LS phase is accessible between 2.645 and 2.670 a.u. In the range between 2.645 and 2.66 a.u., the metamagnetic extensions of both HS and LS phases are accessible. The heavy dashed line specifies the moments at the critical field values. The zero-pressure point is labeled $\times$.

ble in the range between 2.670 and 2.685 a.u. In this range, behavior similar to that depicted in Fig. 4(d) is predicted. Figure 7 also shows three distinct ranges of metamagnetic behavior. The most important is the range from 2.56 to 2.66 a.u. where the metamagnetic extension of the HS phase can be reached with the application and maintenance of a field. Likewise, the range from 2.645 to 2.670 a.u. corresponds to the metamagnetic extension of the LS phase. In the range from $r_{WS}=2.645$ to 2.660 a.u., the metamagnetic extensions of both the HS and the LS phases are accessible and the $M(H)$ curve displays four critical fields (all positive), two for increasing and two for decreasing H. In this range, the NM phase is the only stable phase ($H=0$). Note that a metamagnetic transition from the NM to a stable HS phase is not allowed in fcc Fe. The range from the upper terminus (2.685 a.u.) of the LS phase to $r_{WS}\simeq 2.74$ a.u. is only of theoretical interest. The $M(H)$ curves in this range resemble Fig. 4(d) with all three critical fields negative. The portion representing the metamagnetic extension (to larger volumes) of the LS phase curve, with negative dM/dV, is not accessible because the lower critical field is less negative than the upper critical field. In this range, the HS phase is the only stable phase. We again note that all curves specifying the zero-field moments, and the moments at the critical fields, terminate with infinite dM/dV.

Binding surfaces have also been determined for bcc Co (Ref. 11) and fcc Ni (FM at all r_{WS} studied) and for bcc Ni. The phase information for bcc Co and fcc Ni is relatively uninteresting with the $H=0$ contour showing a smooth variation of magnetic moment with r_{WS} values and showing no volume range capable of sustaining the NM phase (similar to bcc Fe shown in Fig. 5). The equilibrium point corresponds to $r_{WS}=2.605$ a.u. and $M=1.68\mu_B$ for bcc Co and to $r_{WS}=2.58$ a.u. and $M=0.60\mu_B$ for fcc Ni. Figure 8 gives the phase information for bcc Ni and shows that the NM phase is stable below and that the FM phase is stable above $r_{WS}\simeq 2.60$ a.u. with no significant range capable of supporting both phases. For Ni, the equilibrium point for the fcc form (FM) is approximately 4 mRy lower in energy than the equilibrium point for bcc form (NM).

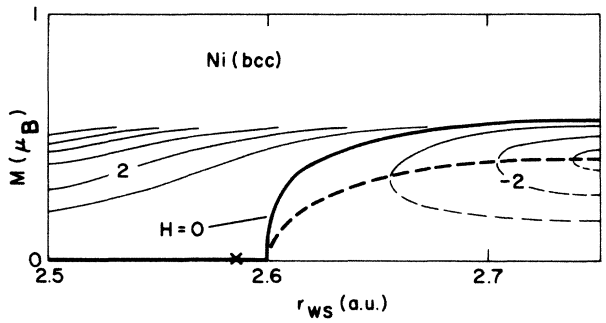

FIG. 8. Constant field contours for bcc Ni exhibiting a stable NM phase below and a stable FM phase above $r_{WS}\simeq 2.60$ a.u. The heavy dashed line specifies the moments at the critical field values. The zero-pressure point is labeled $\times$.

IV. ENERGY VERSUS VOLUME

Another way of displaying pertinent phase information is to show total energies versus volume (or r_{WS}) along phase lines, or lines corresponding to minimum energies for fixed volumes. Although such a presentation is reminiscent of binding curves, we note significant confusion in magnetic E versus V curves presented in the literature. In particular, curves which are labeled nonmagnetic are usually curves obtained by *constraining* the system to be, in fact, nonmagnetic. Such curves correspond to E versus V for the $M=0$ slice of our binding surfaces, but do not show where the NM phase ends, i.e., where d^2E/dM^2 changes sign. In addition multiple phases are often found only with difficulty by conventional spin-polarized (floating moment) methods. Calculations in such multiphase ranges have convergence difficulties and the results are difficult to quantify. In our case the results are unambiguous and clear. Figure 9 displays this information for bcc and fcc Fe (over a pressure range from approximately -250 to $+1200$ kbar), allowing a direct comparison of the two structural forms. We first note that at $P=0$, the bcc FM phase is slightly more favored than the fcc NM phase, in agreement with experiment.[17] The curve for NM fcc Fe extends up to $r_{WS}=2.685$ a.u. At larger r_{WS}

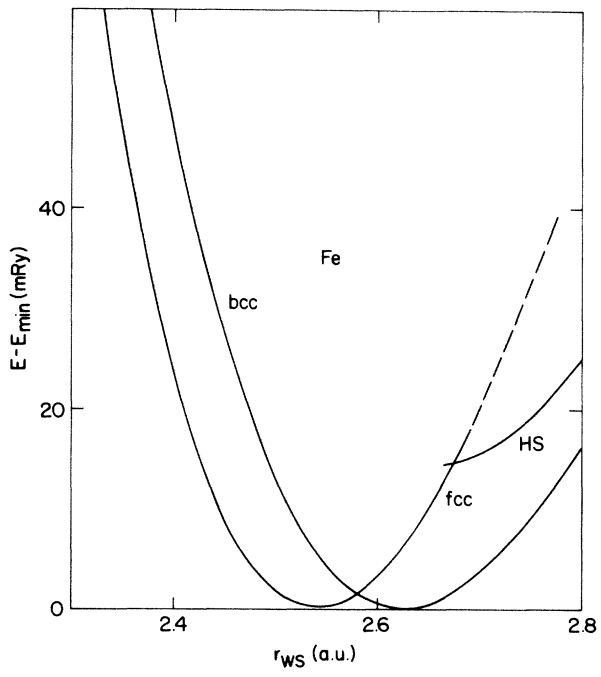

FIG. 9. Total energy (relative to a common minimum energy) vs r_{WS} for bcc and fcc Fe. The ferromagnetic (FM) bcc phase is slightly more favored than the nonmagnetic fcc phase, in agreement with experiment. The FM bcc phase is stable throughout the r_{WS} range considered. In the fcc form, the NM phase is stable for $r_{WS}\leq 2.685$ a.u. and a HS phase is stable for $r_{WS}\geq 2.66$ a.u. The dashed portion of the fcc curve corresponds to the $M=0$ slice of the binding surface and therefore does not correspond to a stable phase. The low-spin phase (LS) is not resolved here but is shown in Fig. 10 where the energy and r_{WS} scale is expanded.

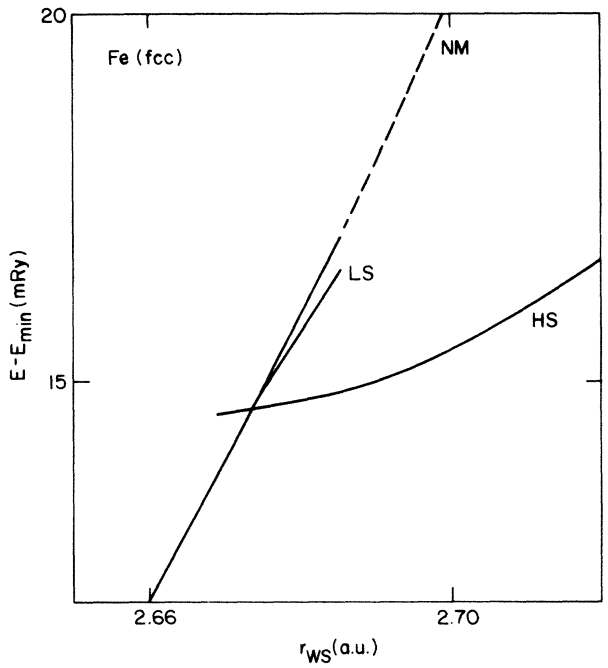

FIG. 10. Total energy vs r_{WS} is the coexistence range for fcc Fe. The high-spin (HS) and low-spin (LS) phases are clearly resolved, with the LS phase having the higher total energy.

values, this NM phase is not stable and is shown dashed. This curve corresponds to the $M=0$ slice of the binding surface shown in Fig. 2. The HS phase corresponding to the trough in the binding surface begins at $r_{WS}=2.66$ a.u. and extends to the largest r_{WS} values considered. The LS phase, shown in Figs. 3 and 7, is barely perceptible on this curve. However, an enlarged view of this region shown in Fig. 10 shows the LS phase lying above the HS phase and extending from 2.670 to 2.685 a.u.

V. DISCUSSION

Our results on fcc Fe can be directly compared with those of Kübler[14] and of Wang, Klein, and Krakauer[18] (WKK), who both found evidence of HS and LS phases. Kübler shows a LS phase extending from $r_{WS}=2.5$ to 2.64 a.u., and a HS phase at larger r_{WS} values and finds that the total energy for the HS phase is everywhere higher than for the LS phase; his curve labeled NM corresponds to a constrained nonmagnetic calculation so that the stability limit cannot be deduced. In later work,[19] Kübler makes no reference to the LS phase. The WKK results show the coexistence of a HS and a LS phase between $r_{WS}=2.66$ and 2.68 a.u., in good agreement with our work, but both Kübler and WKK show a long tail for the LS phase down to $M=0$ at $r_{WS}=2.55$ a.u., which is conspicuously absent in our fixed spin-moment results. We also note that the work of Bagayoko and Callaway[20] (BC) failed to resolve the different magnetic phases for fcc Fe, but showed a smooth $M(V)$ curve and a rapid change in the magnetic moment in the vicinity of $r_{WS}=2.7$ a.u. This behavior is indirect evidence for the existence of multiple phases in this vicinity.

Despite the fact that WKK include non-muffin-tin effects and a more recent form of the local-density approximation, it is interesting to note that they find that fcc Fe is more stable than bcc Fe, in conflict with experiment and the result of the present work. The WKK fcc minimum is 6 mRy lower than the bcc minimum and lattice constants and magnetic moments of the bcc phase disagree with experiment by about 3%. Two possible ways of accounting for this 6-mRy discrepancy between WKK and our results are the following. (1) Inadequate convergence in the **k**-space integration. When the number of points in **k** space is reduced, we find that the bcc minimum energy rises *and* that the fcc minimum energy falls. Hathaway, Jansen, and Freeman[21] also find a rise in the bcc minimum when the number of points in **k** space is reduced, amounting to 6 mRy for a decrease from 210 to 30 points (WKK use 40 points). (2) WKK find a lower moment of $2.08\mu_B$ for bcc Fe compared to our value of $2.15\mu_B$, which corresponds to a smaller magnetic energy and hence a rise in the bcc energy relative to the nonmagnetic fcc energy (they use the local-spin-density approximation of Vosko, Wilk, and Nusair[22]). These sources of discrepancy should be examined further.

The major significance of the present study is the clear resolution of the different ferromagnetic phases of bcc and fcc Fe, Co, and Ni as shown by the discontinuous changes in magnetic moment with volume and by the display of multiphase volume ranges. In the multiphase regions, the description of these simple elemental magnetic systems is shown to resemble the metamagnetic behavior of Stoner's collective electron theory, and the present work essentially provides a first-principles approach to the theory without the introduction of empirical parameters. The results demonstrate the utility of the fixed spin-moment method and, we believe, demonstrate the validity of both the local-spin-density and the muffin-tin approximations used in the study. The results also suggest a variety of experiments on thin films, epitaxially "clamped" at selected lattice separations. We note, in particular, (1) the prediction of a nonmagnetic bcc phase of Ni which is only 4 mRy less stable than the ferromagnetic fcc phase, and which is expected to become ferromagnetic at a 1% lattice expansion, (2) the prediction that fcc Fe is only slightly less stable than bcc Fe, and exhibits NM, LS, and HS phases at approximately a 5% lattice expansion, and (3) the prediction of a NM phase for fcc Co at a 4% lattice compression.

[1]W. Kohn and L. Sham, Phys. Rev. **140**, A1133 (1965).
[2]V. L. Moruzzi, J. F. Janak, and A. R. Williams, *Calculated Electronic Properties of Metals* (Pergamon, New York, 1978).
[3]O. K. Andersen, J. Madsen, U. K. Poulsen, O. Jepsen, and J. Kollar, Physica **86&88B**, 249 (1977).
[4]D. M. Roy and D. G. Pettifor, J. Phys. F **7**, L183 (1977).
[5]A. R. Williams, V. L. Moruzzi, J. Kübler, and K. Schwarz, Bull. Am. Phys. Soc. **29**, 278 (1984); K. Schwarz and P.

Mohn, J. Phys. F **14**, L129 (1984). In this work we only consider ferromagnetic order. The fixed spin-moment method has not yet been extended to the more complicated problem of antiferromagnetic order.

[6]P. H. Dederichs, S. Blügel, R. Zeller, and H. Akai, Phys. Lett. **53**, 2512 (1984).

[7]A. R. Williams, J. Kübler, and C. D. Gelatt, Jr., Phys. Rev. B **19**, 6094 (1979).

[8]U. von Barth and L. Hedin, J. Phys. C **5**, 1629 (1972).

[9]J. F. Janak, Solid State Commun. **25**, 53 (1978).

[10]V. L. Moruzzi, Thesis, Technical University of Vienna, Vienna, Austria, 1985. See also, P. M. Marcus and V. L. Moruzzi, Solid State Commun. **55**, 971 (1985).

[11]V. L. Moruzzi, P. M. Marcus, K. Schwarz, and P. Mohn, J. Magn. Magn. Mater. **54-57**, 955 (1986).

[12]P. M. Marcus, V. L. Moruzzi, and K. Schwarz, in *Computer-based Microscopic Description of the Structure and Properties of Materials,* Vol. 63 of *Materials Research Society Symposia Proceedings,* edited by J. Broughton, W. Krakow, and S. T. Pantelides (Materials Research Society, Pittsburg, 1986).

[13]G. A. Prinz, Phys. Rev. Lett. **54**, 1051 (1985).

[14]J. Kübler, Phys. Lett. **81A**, 81 (1981).

[15]E. P. Wohlfarth and P. Rhodes, Philos. Mag. **7**, 1817 (1962); M. Shimizu, J. Phys. (Paris) **43**, 155 (1982).

[16]The model of magnetic behavior used here only includes spin magnetization, which requires the moment to be parallel or antiparallel to the applied magnetic field. Negative fields, i.e., fields opposite to the direction of the moment, can be tolerated in the ferromagnetic state because the model provides an energy barrier to reversing the magnetization direction. When a threshold negative field is exceeded, the system will abruptly assume the opposite magnetization. Mechanisms outside the model, e.g., rotation of the spin direction, may permit spin reversal at smaller threshold fields.

[17]At the crossing point of the fcc and bcc curves in Fig. 9, which is where a transition to the fcc state would take place if the transition occurred at constant volume, the pressure in the bcc state is 140 kbar. The (extrapolated) experimental phase diagram for Fe indicates a transition at $T=0$ from bcc to hcp (α to ϵ) at about 140 kbar; [see Lin-gun Liu and L. H. Bassett, J. Geophys. Res. **80**, 3777 (1975)].

[18]C. S. Wang, B. M. Klein, and H. Krakauer, Phys. Rev. Lett. **54**, 1852 (1985).

[19]J. Kübler, in the Proceedings of the Institute von Laue-Langevin Workshop on 3*d* Metallic Magnetism, Grenoble, France, 1983, edited by D. Givord and K. Ziebeck (unpublished).

[20]D. Bagayoko and J. Callaway, Phys. Rev. B **28**, 5419 (1983).

[21]K. B. Hathaway, H. F. J. Jansen, and A. J. Freeman, Phys. Rev. B **31**, 7603 (1985).

[22]S. H. Vosko, L. Wilk, and M. Nusair, Can. J. Phys. **58**, 1200 (1980); S. H. Vosko and L. Wilk, Phys. Rev. B **22**, 3812 (1980).